Mon. Not. R. Astron. Soc. **000**, 1–?? (2004) Printed 10 March 2010 (MN LaTeX style file v2.2)

arXiv:1003.1893v1 [astro-ph.IM] 9 Mar 2010

The Infrared Astronomical Characteristics of Roque de los Muchachos Observatory: precipitable water vapor statistics

B. García-Lorenzo[1,2]⋆, A. Eff-Darwich[3], J. Castro-Almazán[1], N. Pinilla-Alonso[4], C. Muñoz-T
1 Instituto de Astrofísica de Canarias, C/Via Lactea S/N, 38305-La Laguna, Tenerife, Spain
2 Dept. Astrofísica, Universidad de La Laguna, C/ Astrofísico Francisco Sánchez, E-38205 Tenerife, Spain
3 Dept. Edafología y Geología, Universidad de La Laguna, C/ Astrofísico Francisco Sánchez, E-38205 Tenerife, Spain
4 NASA Ames Research Center, MS 245-3, Moffet Field, 94035-1000, CA

Accepted ..... Received .....; in original form .....

ABSTRACT

The atmospheric water vapor content above the Roque de los Muchachos Observatory (ORM) obtained from Global Positioning Systems (GPS) is presented. GPS measurements have been evaluated by comparison with 940nm-radiometer observations. Statistical analysis of GPS measurements points to ORM as an observing site with suitable conditions for infrared (IR) observations, with a median column of precipitable water vapor (PWV) of 3.8 mm. PWV presents a clear seasonal behavior, being Winter and Spring the best seasons for IR observations. The percentage of nighttime showing PWV values smaller than 3 mm is over 60% in February, March and April. We have also estimated the temporal variability of water vapor content at the ORM. A summary of PWV statistical results at different astronomical sites is presented, recalling that these values are not directly comparable as a result of the differences in the techniques used to recorded the data.

Key words: Site Testing — Infrared: General — Instrumentation: miscellaneous

1 INTRODUCTION

The triatomic molecules H_20, CO_2 and O_3 are the main responsible for reducing the few transparent windows on the infrared atmospheric transmission spectrum, and producing absorption bands that are difficult to correct during the processing of astronomical data. Out of these windows, the atmosphere is opaque and observations at those wavelengths have to be carried out from space. Sites with large atmospheric water vapor levels have narrow and unstable transparent windows. High levels of water vapor reduce the atmospheric transparency, but also increase the thermal infrared background.

It is assumed among the astronomical community that sites placed at lower altitudes are less suitable for high-quality IR observations; however, other parameters such the troposphere thickness might be also playing an important role (García-Lorenzo et al. 2004). Indeed, the evaluation of the IR quality at the Observatorio del Teide in the Canary Islands, Spain (Mountain et al. 1985) and the comparison with prediction models (Cohen et al. 1992) indicate that El Teide site, at ∼2400 m above sea level, might be as good as Mauna Kea (4200 m) for IR astronomy in the 1-5 μm window (Hammersley 1998). Observational results pointing to a similar conclusion were reported for Roque de los Muchachos observatory (ORM) on the island of La Palma (Canary Islands, Spain), also at ∼2400 m above sea level, when comparing infrared observations from the 3.58m Telecopio Nazionale Galileo with data obtained at the 10m Keck telescope on Mauna Kea astronomical observatory (Hawaii, USA) (http://www.tng.iac.es/news/2003/03/21/nics_refurbish).

There are many parameters accounting for the quality of an astronomical site, namely seeing, cloud cover, ground winds, high-altitude winds, etc (see Muñoz-Tuñón et al. (2007) for a review on the characterization of these parameters at ORM). The water vapor content is an important parameter affecting the IR quality of astronomical sites. Conditions for IR astronomical observations were classified in terms of precipitable water vapor (PWV hereafter) in four divisions (Kidger et al. 1998): 1) Good or excellent → $PWV \leqslant 3$ mm; 2) Fair or mediocre → $3 < PWV \leqslant 6$ mm; 3) Poor → $6 < PWV \leqslant 10$ mm; and (4) Extremely poor → $PWV \geqslant 10$ mm . The development of IR instrumentation and the requirements for current large and future extremely large telescopes demand a proper characterization of PWV and statistical studies of large temporal databases (covering years). The fraction of nights with good IR conditions (small

---

⋆ E-mail: bgarcia@iac.es

column of water vapor) as a function of the epoch of the year will allow an optimal scheduling of telescope observing time. The total atmospheric water vapor contained in a vertical column of unit cross-sectional area extending between any two specified levels is known as precipitable water vapor and it is commonly expressed in terms of the height to which that water substance would stand if completely condensed and collected in a vessel of the same unit cross section (American Meteorological Society 2000). PWV is also referred to as the total column water vapor (Ferrare et al. 2002). Measurements of PWV can be obtained in a number of ways, from *in situ* measurements (radiosondes) to remote sensing techniques (photometers, radiometers, GPS, Imaging Spectroradiometers on satellites, etc). Radiosondes have been the primary *in situ* observing system for monitoring water vapor; however, the operability of radiosondes is limited due to running costs and decreasing sensor performance in cold dry conditions (Li et al. 2003). Usually, radiosondes are expected to measure PWV with an uncertainty of a few millimetres, which is considered to be the standard accuracy of PWV for meteorologists (Niell et al. 2001). Near infrared (NIR) radiometers measuring methodology assumes plane-parallel atmosphere, hence it is only satisfactory for measurements near the Zenith. Moreover, their uses are limited to photometric and bright nights (from first quarter to last quarter Moon). Errors of 20% or below are estimated for PWV measurements using NIR radiometers in the range 3-10 μm, whereas errors in the 0.5-1μm range might be as high as 40% (Quesada 1989). Microwave water vapor radiometers (WVR) observations are not reliable when liquid water is present on the WVR frequency window (Liou et al. 2001) or when there is significant scattering from liquid water droplets and ice crystals in the field-of-view (Zhang et al. 1999).

GPS is an increasingly useful tool for measuring PWV, which has gained a lot of attention in the meteorological community. The GPS procedure to estimate the PWV is based on the fact that the propagation of electromagnetic waves through the atmosphere is drastically affected by variations on the refraction index of the troposphere, which depends on the water vapor pressure, air pressure, and temperature. The consequence is an induced delay in any signal crossing the atmosphere, being due to a combination of a hydrostatic and a water vapor delay. The hydrostatic delay is very stable and has a direct relationship with local atmospheric pressure. The second component, the wet delay, is directly related to the water vapor content in the atmosphere above the site where the measurements are taken. The rapid temporal variations of the water vapor affects its prediction and proper measurement. The overall tropospheric delay at a GPS station allows the estimation of the PWV with a high-degree of accurancy (Bevis et al. 1994; Boccolari et al. 2006; Jin et al. 2009), although under very dry environments GPS might underestimate the PWV content (Schneider et al. 2009). GPS system provides a better spatial coverage and continuous PWV estimations in comparison with other techniques (Ge et al. 2000). The comparison of GPS, radiosondes and WVR (Emardson et al. 2000; Niell et al. 2001; Li et al. 2003) shows agreement generally at the level of 1-2 mm of PWV, corresponding to 7-13 mm of zenith wet delay (error << 10%).

In this paper, we present statistical results on the PWV above the Roque de los Muchachos Observatory (La Palma, Spain) derived from GPS measurements for the period spanning from June 2001 to December 2008. For comparison purposes, we also present PWV statistical results for Mauna Kea site derived also from GPS data.

2 DATA SOURCES

2.1 PWV measurements at ORM

The Roque de los Muchachos Observatory is located at an altitude of 2396 m above sea level on the island of La Palma (Canary Islands, Spain) at latitude 28^0 45 North and longitude 17^0 53 West. This observatory is one of the final candidate sites for the location of the 42 m European Extremely Large Telescope. The Spanish Instituto Geográfico Nacional has installed permanently since May 2001 a GPS receiver at ORM. The GPS antenna is placed on a very stable monument which ensures that the GPS satellite data recorded at the station does not contain any spurious antenna movement that could affect the scientific exploitation of the GPS data. This permanent GPS is part of the international network – *European Reference Organisation for Quality Assured Breast Screening and Diagnostic Services* (www.euref.eu) – of GPS stations (Kenyeres & Bruyninx 2004). The data from the GPS station at the ORM for the period spanning from June 2001 to December 2008 were processed by Soluciones Avanzadas Canarias S.L. (www.sacsl.es), a company devoted to GPS data processing for the International Global Navigation Satellite Systems Service (Romero et al. 2003). Global GPS data were processed using the dual frequency data recorded at around 35 stations worldwide including the station at ORM. The daily data processing runs take data from each station using all the data available above 10 degrees of elevation at each ground station every 5 minutes (epoch). The satellite orbits are considered fixed as downloaded from the International Global Navigation Satellite Systems Service (www.igs.org). The Tropospheric Zenith Delay (TZD) for each station is estimated every two hours with an initial value of 2.1 meters and an a-priori sigma of 2 meters, hence being considered "free". The long standing stations have coordinates/velocities published in the International Terrestrial Reference Frame (Altamimi et al. 2007) which are very precise and can be kept almost fixed. The coordinates for the stations in study are estimated using the initial conditions with a 3 mm a-priori sigma. This allows the coordinate estimation to be adjusted slightly over the processing arc to accommodate small daily variations from the published International terrestrial reference frame positions.

In each observation epoch, each station has measurements to all the satellites in-view. Nominally each station records measurements to 8-12 satellites per epoch. This means that for the TZD estimation (one value every two hours per station) each TZD value is averaged over 24 epochs (5-minutes each). Therefore, more than $\sim$ 200 individual measurements (24 epochs × 8-12 satellites) contribute to the TZD estimation. A two-hour averaging time is standard in GPS processing for TZD, although shorter estimations can be performed. More details on the theoretical basis for the ground-based GPS technique, the background physics and potential applications can be found in e.g. Bevis et al.

(1992). The accuracy of GPS measurements are not limited by the system receiver noise, but largely by modeling errors. The uncertainties of the system are multidimensional, including errors from satellite orbits, errors in the mapping functions used for the atmosphere delay estimations, scattering in the vicinity of the GPS antenna, the effect of any radome in the antenna, etc. An introduction and description of GPS data processing can be found, for example, in Blewitt (1998) or Leick (2004).

The TZD derived from the GPS data processing is composed of two contributions, the hydrostatic (ZHD) and the wet (ZWD) delays. The ZHD can be calculated through the latitude (ϕ in degrees), altitude (H in meters) of the GPS station (Saastamoinen 1973, 1972) and the atmospheric pressure (P in hPa) according to the following expression:

$$ZHD = \frac{22.768 \times 10^{-4} \times P}{1 - 26.6 \times 10^{-4} cos(2\phi) - 0.28 \times 10^{-6} \times H} \quad (1)$$

The ZWD accounts for the PWV in the atmosphere and can be derived by subtracting ZHD from the TZD value. PWV can be then calculated as a proportion of the estimated ZWD through the following equation (Askne & Nordius 1987):

$$PWV = ZWD \times \frac{10^6}{\rho R_V[(k_3/T_m) + k_2]} \quad (2)$$

where ρ is the density of liquid water, R_V is the specific gas constant for water vapor, k_2=70.4 K mbar^{-1}, k_3=3.739 10^5 K^{2}mbar^{-1} are the refractivity constants (Bevis et al. 1994; Askne & Nordius 1987), which have been determined by direct measurements using microwave techniques (see Bevis et al. (1994) for more details on these constants). T_m is a weighted mean temperature of the atmosphere, which is strongly correlated with surface temperature (T_s) according to the linear relation (Bevis et al. 1992):

$$T_m = 70.2 + 0.72T_s \quad (3)$$

The uncertainties in the refractivity coefficients of the water vapor and the selected mapping functions in the TZD calculation can introduce a scale factor in the PWV derived from GPS measurements (Niell et al. 2001). Therefore, the comparison of PWV estimations from GPS data with other techniques will require an initial model consisting of a scale factor between techniques and an offset accounting for a bias in the measurements. This bias comes from residual delays that are estimated as corrections to a delay model assuming a standard atmosphere using a zenith angle dependent mapping function (Kleijer 2001). The estimation of the PWV from TZD derived by GPS measurements requires surface pressure and temperature measurements. The ZWD will not include an additional bias if accurate surface pressure is used in the estimation of ZHD. Unfortunately, there is not a weather station at the precise location of the GPS antenna at ORM; hence a model (Boehm et al. 2007) of the pressure and temperature at the longitude, latitude and height of the station for each date was used to obtain PWV from the derived TZD using equation 1, 2, and 3. The GPS time series for ORM consist of more than 31500 individual estimations with a two-hour temporal resolution of the PWV for the period June 2001 to December 2008.

During the site prospection for the emplacement of the 10 meters Gran Telescopio de Canarias, different campaigns of PWV measurements above ORM were carried out from February 2000 to July 2002 using a two band radiometer. The radiometer operates in the 940-nm water vapor band (Kidger et al. 1998, 2002; Pinilla et al. 2002; Pinilla 2003). Observations were taken on the Moon (solar observations are also possible including an appropiated neutral density filter), measuring the entire 940-nm water vapor absorption line (filter centered on 946.7 nm with a bandwidth of 19.8 nm) and nearby continuum (filter centered on 884.5 nm with a bandwidth of 18.2 nm). The PWV is directly correlated to the square of the ratio of the signal in the two filters. No model-dependent assumptions are made for this calculation. The absolute calibration of the 940nm-radiometer was measured from radiosonde flights for a range spanning from 0.5 to 25 mm of water vapor. This remote sensing technique assumes a plane-parallel atmosphere, restricting the measurements to nearly Zenithal positions (Quesada 1989; Gao et al. 1993) in order to convert the measured line-of-sight PWV to the zenithal values. The relative precision of the line-of-sight PWV is around 5% for a single measurement (Kidger et al. 1998). The two main drawbacks of this technique are that is only usable in photometric conditions and with the Moon well above the horizon. 940nm-Radiometer required a human supervision and the temporal resolution was about 30 minutes.

A direct comparison between GPS and the 940nm-radiometer could be carried out for the period from June 2001 to July 2002. In this sense, 243 PWV estimations from the 940nm-radiometer were recorded. In order to perform the comparison, we re-sampled the 940nm-radiometer dataset to the same temporal resolution of the GPS data. Following the temporal re-sampling, the number of data was reduced to 55 in both the GPS and the radiometer. As we already mentioned, errors up to 40 % has been reported for PWV estimations when using radiometer measurements in the 0.5-1 μm range (Quesada 1989). We have adopted the standard deviation of the averaged 940nm-radiometer data in the two-hour sampling as the error of the PWV estimation, being smaller than 25% for all the estimations. Errors of about 1 mm are estimated for the PWV derived from the proccesing of the GPS data. We obtained a good correlation between GPS and 940nm-radiometer measurements of PWV for the period June 2001-July 2002 (Fig. 1), with a Pearson correlation coefficient of 0.97. A linear relationship was determined using the task LINMIX_ERR (Kelly 2007), available from the IDL Astronomy User's Library, which incorporates a Bayesian approach to linear regressions taking into account measured errors on both variables. The best-fit relation and the residuals of the best-fit are shown in Figure 1. The standard deviation of these residuals is 1.5 mm. The linear regression gives a scale factor of 0.9±0.1, with an offset at zero of -1.2±0.1 mm.

The 940nm-radiometer provided the statistical values taken as representative of the ORM site until now. Therefore, we adopted the 940nm-radiometer as the reference instrument to calibrate the long-term GPS time series in order to compensate the scale and offset errors introduced in the data processing. The standard deviation of the residuals was chosen as the uncertainty associated to the PWV estimations from the GPS measurements at ORM. Figure 2 presents the full time series of PWV data derived from GPS measurements above ORM in the period from June

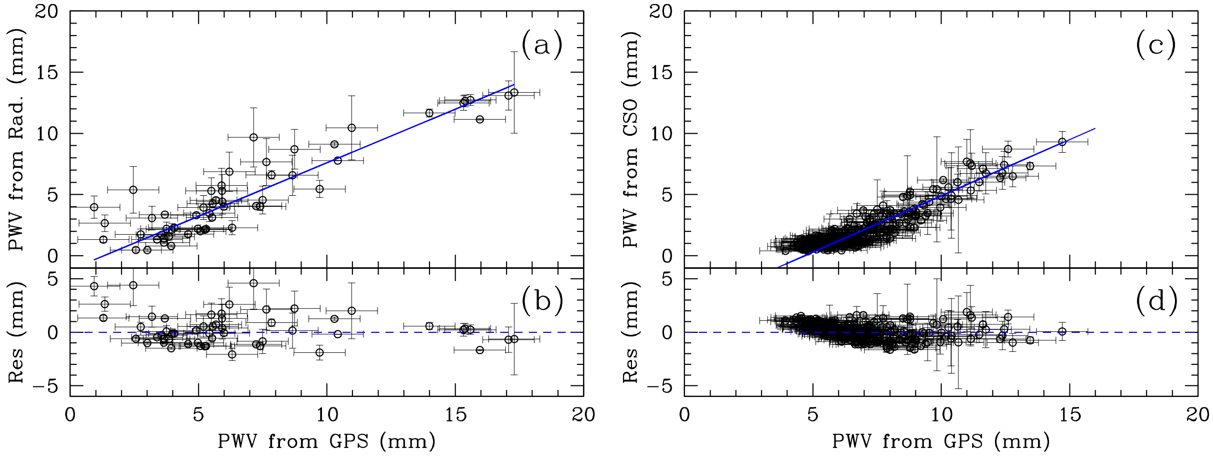

Figure 1. Comparison of PWV estimations from GPS and : (a)-(b) 940nm-radiometer measurements at La Palma site; (c)-(d) PWV estimations from atmospheric opacity at 225 GHz at Mauna Kea site. (a) and (c) The solid line corresponds to the best fit derived from a Bayesian approach to linear regressions with errors in both variables (Kelly 2007). (b) and (d) The residuals of the best-fit model.

2001 to December 2008. This figure also includes the fraction of measurements for which PWV was found to be below a given value.

Unlike other techniques, GPS provides PWV estimations in nearly all atmospheric conditions, including those of local fog, dust and/or presence of clouds (non-photometric conditions). These conditions will induce large PWV values that are not considerered in PWV time series obtained from 940nm-radiometer measurements.

2.2 PWV data at Mauna Kea

Mauna Kea is an excellent astronomical site for thermal IR observations. The Caltech Submillimeter Observatory (CSO) has two monitors (Latitude 19.8224995 North, Longitude -155.475844 West; Altitude: 4070 m above sea level) of atmospheric opacity, one operating at 225 GHz and another at a wavelength of 350 μm permanently installed since the nineties. The characteristics of these radiometers have been extensively described (Liu 1987; McKinnon 1987; Chamberlin & Bally 1994). More information about these monitors is provided in the CSO Tau monitor webpage (http://puuoo.submm.caltech.edu/). Previous work (Davis et al. 1997) has shown that the atmospheric opacity at 225 GHz, τ_{225GHz}, is related to the column abundance of water vapor in mm, namely:

$$PWV = 20 \times (\tau_{225GHz} - 0.016) \qquad (4)$$

The time series of τ_{225GHz} measurements above Mauna Kea were collected from the CSO archive for the period June 2001 to December 2008. The temporal sampling of τ_{225GHz} is about 10 minutes. The PWV was estimated (PWV_{225GHz} hereafter) from τ_{225GHz} data using equation 4. Statistical results based on this reference PWV_{225GHz} time series have been already presented (García-Lorenzo et al. 2009; Otárola et al. 2010).

A permanent GPS station (labelled MKEA) is located (Latitude:19.8014 North, Longitude:-155.456 West and Altitude: 3755 m above sea level) at approximately 4 km from Mauna Kea observatory. The coordinate estimation per process for the GPS antenna at MKEA produces height estimates which are very consistent day to day. This confirms that the station is correctly installed, stable and that the data is relevant in this scientific context for water vapor estimations. It is important to point out that the statistical results from PWV derived using these GPS data might not be representative of the PWV conditions at Mauna Kea astronomical site as the GPS station is four km distant from the observatory, although we assume hereafter a similar behavoiur of the PWV in both locations. The difference in altitude between Mauna Kea site and the GPS ($\sim 315m$) might introduce an aditional bias in the PWV estimations derived from GPS relative to the values obtained from τ_{225GHz}. This bias could be up to 1 mm assuming a similar variation of PWV with height as the found in Atacama sites (Giovanelli et al. 2001) or in Pico Veleta (Quesada 1989). The data from the MKEA GPS station for the period June 2001-December 2008 were proccessed using the same global GPS data procedure that we used for the GPS station at La Palma site. In order to compare the GPS time series estimations of PWV to PWV_{225GHz}, the CSO Tau monitor is adopted as the reference instrument. The PWV_{225GHz} data were re-sampled to the same temporal resolution of the GPS time series (2 hours). The standard deviation of the averaged PWV_{225GHz} in the two-hour sampling is taken as the error of each measurement. Errors of about 1 mm are assumed for the PWV derived from the proccesing of the GPS data (PWV_{GPS} hereafter). The number of data to be compared is 20880. The Pearson correlation coefficient obtained when comparing PWV_{GPS} and PWV_{225GHz} is 0.91. Several random selections of about 500 data were performed in order to apply the same Bayesian approach to linear regressions than that used for La Palma data. The result of the linear regression gives a scale factor of 0.9±0.1 and an intercept of -4.3±0.1 mm (Fig. 1). This offset comes from a combination of modeling errors in the GPS treatment and the difference in altitude between the GPS station and the CSO Tau monitor. These scale and offset factors were applied in order to compensate the already explained errors (section §2.1) introduced in the GPS data processing. The standard

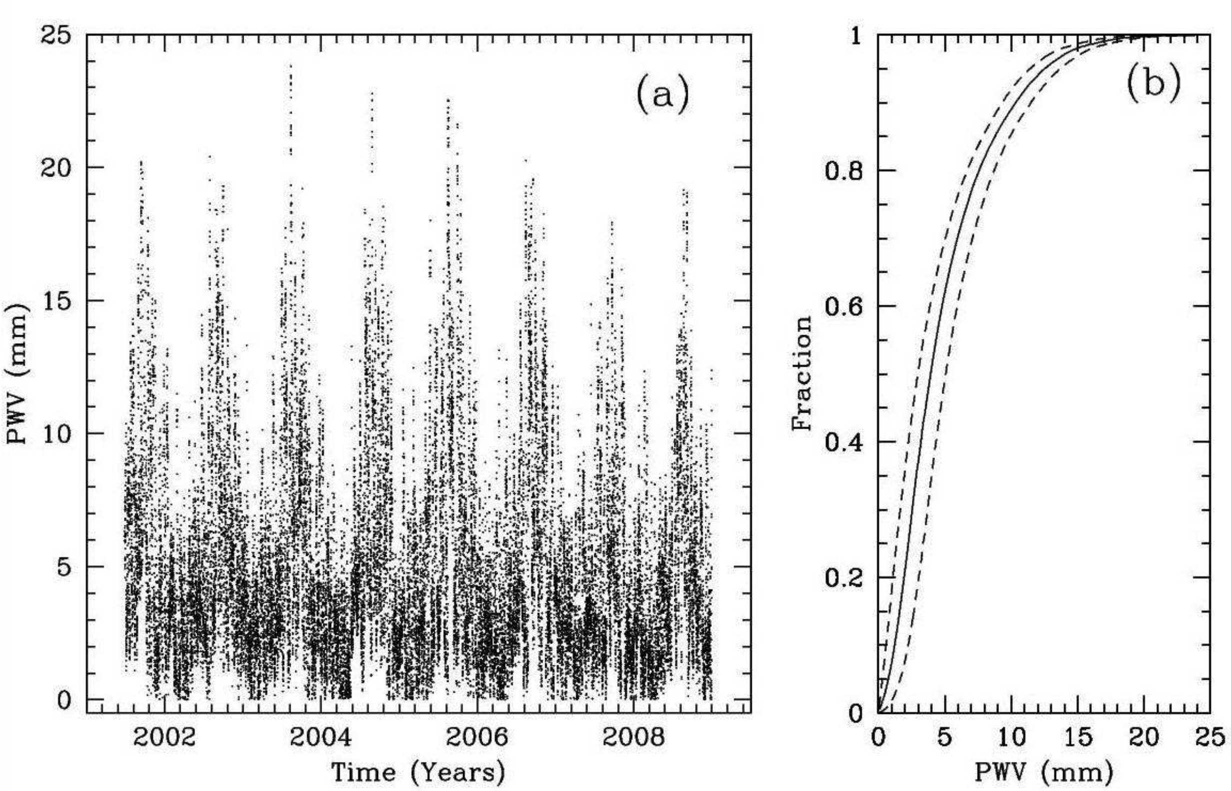

Figure 2. (a) The two-hourly time series of PWV estimations from GPS measurements at ORM from June 2001 to December 2008. (b) Cumulative distribution of PWV measurements (solid line) above ORM. Dotted lines represent the uncertainties due to both the measurements and the calibration.

deviation of the residuals to the linear approach is 1.6 mm, which it is assumed hereafter as the uncertanties associated to PWV derived from GPS data at Mauna Kea. The full time series of PWV from GPS measurements obtained for MKEA in the period from June 2001 to December 2008, and the cumulative distribution of the measurements are shown in Figure 3.

3 ANALYSIS AND RESULTS

GPS measurements provide PWV estimations almost continuously, including daytime and nighttime data. The average PWV at ORM was 4.9 mm, with an standard deviation of 3.7 mm. The median value considering all the estimations in the PWV time series for ORM is 3.9 mm (Table 1). Ephemerides from the Nautical Almanac of the Real Observatorio de la Armada de San Fernando (http://www.armada.mde.es) has been used to divide the data in day and nighttime series. The average daytime PWV is 5.1±3.7 mm, whereas the average nighttime PWV is 4.8±3.7 mm (Table 1). The uncertainties indicate only the standard deviation of the averaged measurements.

The statistical study of PWV variability at different temporal scales is of relevant importance for an effective scheduling at an astronomical observatory with IR capabilities. We have used the time series of PWV estimations from GPS data above ORM to study the variability of this parameter at seasonal, monthly, and daily scales, but it is important to note that weather patterns are highly variable on all timescales. Variability for periods larger than a year (e.g. associated to North Atlantic oscillation events and/or a global warming) can not be raised with our current 7.5-year time series.

3.1 Daily variations

It is expected that larger temperatures result in larger PWV (as it is expressed in equation 2). Since temperature follows a clear diurnal variation (Yagai 2002), it might be likely that PWV follows a similar trend. The two-hourly time series above La Palma site were used to analyse the variations of PWV in a 24-hour period. The global statistics (Table 1) suggests a slight difference between day and night values of PWV, with larger daytime values. However, such differences between daytime and nighttime seems to not follow a clear daily behaviour, in the sense that the minimum and maximum PWV during a full day does not have a defined period. Indeed, maxima or minima values of PWV might appear at any hour during the day as it is illustrated in Fig. 4. The distribution of the maximum PWV presents two peaks, at around noon and midnight, while the distribution of minimum PWV presents a peak only at around midnight. We have tested that this distribution does not change significatly if we only take into account the days from a particular season or month. Therefore, a clear daily behaviour of the PWV is not found at ORM.

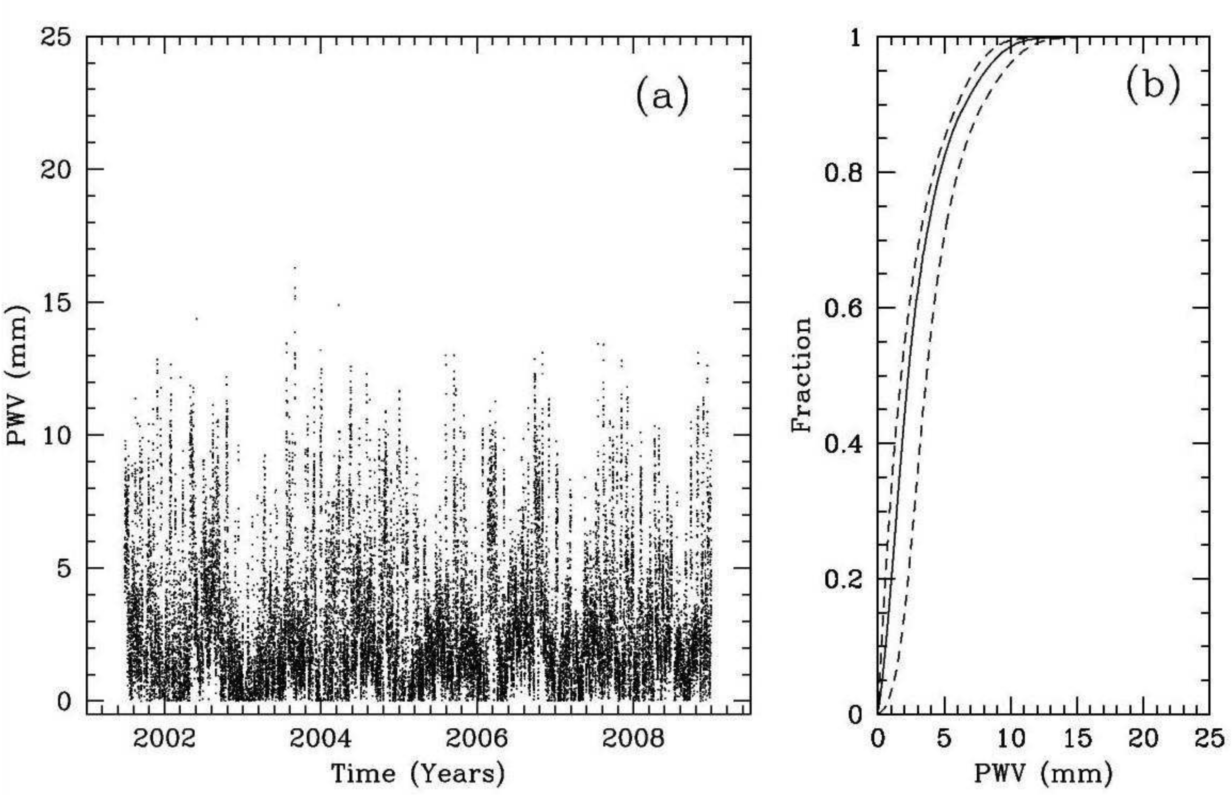

Figure 3. (a) The two-hourly time series of PWV estimations from GPS measurements close to Mauna Kea astronomical site from June 2001 to December 2008. (b) Cumulative distribution of PWV measurements (solid line) above Mauna Kea. Dotted lines represent the uncertainties due to both the measurements and the calibration.

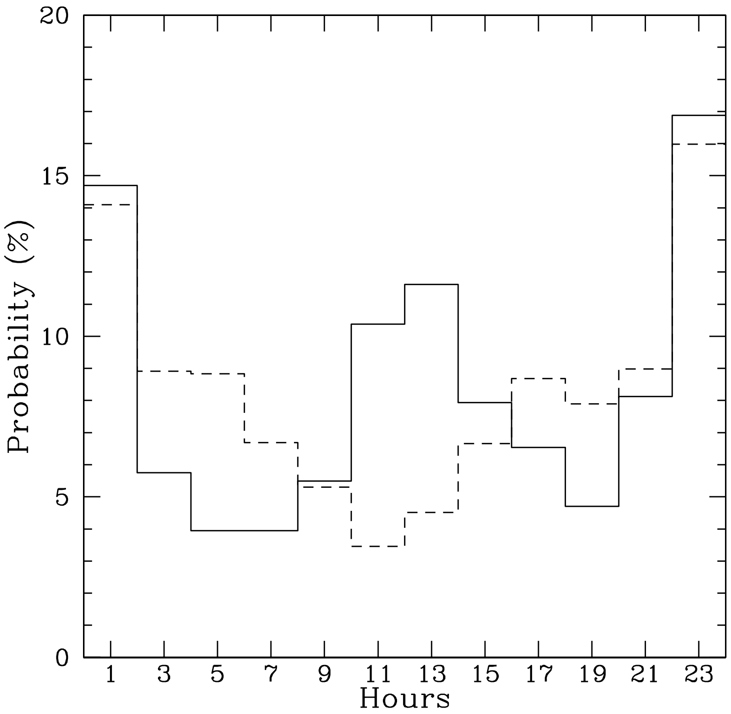

Figure 4. Distribution of hours at which maximum (continuous line) and minimum (dashed line) PWV are reached during a 24-hour period.

Table 1. Global and seasonal statistical results of precipitable water vapor (in mm) above the Roque de los Muchachos Observatory. The percentage of time in which the PWV is within a defined range is also shown.

		Global	**Winter**	**Spring**	**Summer**	**Autumn**
All:						
	Mean	4.9	3.3	3.5	6.7	5.6
	σ	3.7	2.3	2.4	4.3	3.8
	N	30920	6886	7200	8655	8179
	10%	1.2	0.9	0.9	2.0	1.4
	25%	2.3	1.7	1.8	3.2	2.6
	50%	3.9	2.9	3.0	5.7	4.8
	75%	6.7	4.4	4.7	9.4	7.9
	90%	10.3	6.3	6.6	13.0	11.13
All:	**PWV Range**					
	< 2 mm	21%	31%	29%	9%	17%
	2-3 mm	17%	21%	20%	13%	13%
	3-6 mm	33%	36%	37%	30%	31%
	6-10 mm	18%	10%	12%	26%	25%
	$\geqslant$ **10 mm**	11%	2 %	2%	22%	14%
Day:						
	Mean	5.1	3.4	3.6	6.8	5.7
	σ	3.7	2.2	2.3	4.2	3.8
	N	12967	2514	3223	3904	3326
	10%	1.4	1.0	1.0	2.2	1.5
	25%	2.4	1.9	2.0	3.4	2.7
	50%	4.1	3.0	3.2	5.7	4.9
	75%	6.8	4.5	4.9	9.4	8.1
	90%	10.5	6.3	6.8	12.7	11.5
Day:	**PWV Range**					
	< 2 mm	18%	28%	26%	8%	16%
	2-3 mm	17%	22%	20%	12%	14%
	3-6 mm	35%	38%	39%	32%	30%
	6-10 mm	19%	10%	13%	26%	25%
	$\geqslant$ **10 mm**	11%	2%	2%	22%	15%
Night:						
	Mean	4.8	3.3	3.3	6.7	5.7
	σ	3.7	2.3	2.4	4.4	3.7
	N	17921	4340	3977	4751	4853
	10%	1.2	0.8	0.8	1.9	1.4
	25%	2.1	1.6	1.6	3.1	2.6
	50%	3.8	2.8	2.9	5.7	4.7
	75%	6.6	4.4	4.5	9.5	7.8
	90%	10.2	6.3	6.4	13.1	11.0
Night:	**PWV Range**					
	< 2 mm	23%	33%	32%	11%	17%
	2-3 mm	16%	20%	20%	13%	13%
	3-6 mm	32%	35%	35%	29%	31%
	6-10 mm	18%	10%	11%	25%	25%
	$\geqslant$ **10 mm**	11%	2%	2%	22%	14%

3.2 Seasonal variations

We have derived the global and seasonal statistics of PWV for the period June 2001-December 2008 (see Table 1). Seasonal differences in the statistical values for daytime and nighttime PWV were found. The smallest statistical PWV corresponds to winter and spring, wheareas the largest occurs in summer. Table 1 also presents the percentage of time in which PWV lies on a determined range of values defined following the criteria to classify the observational conditions for IR observations in Kidger et al. (1998). Approximately 38% of the time (including day and night) the ORM presents PWV values smaller than 3 mm, this percentage increases to more than 52% for winter and spring nighttime. On the contrary, values larger than 6 mm are found 29% of the total time, although this percentage is only about 12% in winter and spring.

We have also derived the monthly average PWV for the different years and for the full period in order to study in detail the seasonal trend (figure 5). The PWV presents a clear seasonal behaviour, being September and April the statistically worst and best months, respectively, in terms of PWV. The seasonal behaviour does not significantly differ among the years, showing the largest PWV values during August-September and the lowest during March-April. The latter results were also found if we considered separately the daytime or nighttime series. This seasonal behaviour could be related to the seasonal variation of the temperature (see e.g. the yearly temperature graph for ORM at http://catserver.ing.iac.es/weather/archive/mrtg/temp_out.html), as the PWV strongly depends on this meteorological variable. Seasonal trends of the PWV have been also reported for other astronomical sites in both hemispheres (Otárola et al. 2010).

If we only take into account the nighttime series, 39% of the time PWV are lower than 3 mm (table 1). We have calculated the monthly percentage of night time at which the PWV conditions are good or excellent for IR observations, that is PWV $\leqslant$ 3 mm (Figure 6). This percentage also varies along the months. In February, March and April, more than 60% of the nighttime presents high quality conditions to perform IR observations. Even in September, the worst month in terms of PWV, 10% of the nighttime is highly adequated to perfom IR observations. In this sense, high quality IR observations at ORM could be carried out at any time of the year, being April the best month with ∼ 63% of the nighttime presenting PWV $\leqslant$ 3 mm.

3.3 Temporal Stability

Temporal stability is an important property in site-testing analysis (Racine 1996; Muñoz-Tuñón et al. 1997; Skidmore et al. 2009), although it is not usually taken into account. Different astronomical sites with similar average values for a particular parameter could strongly differ in the temporal stability of that parameter. In this sense, the characterization of the temporal evolution of a parameter might be used to optimize the operability of astronomical facilities. The temporal fluctuations of PWV drastically affects the schedule of an observing night at a telescope/observatory working in queue mode. Therefore, estimations of the range of PWV fluctuations on a given time scale is an important factor to take into account for queue-scheduled IR observations. The long-time series of PWV estimations recorded at ORM using a two-hour sampling of GPS measurements allows us to evaluate the temporal variability of the PWV. Variations of PWV in time scales smaller than two hours can not be studied with the current time series.

In order to study the temporal variability of the PWV at the ORM, we have applied the fractional difference (FD) and the absolute difference (AD) methods. The FD method was introduced by Racine (1996) to study the temporal fluctuations of the seeing at Mauna Kea. The FD method is based on a function $f_{FD}(\Delta t)$:

$$f_{FD}(\Delta t) = < \frac{|PWV(t+\Delta t) - PWV(t)|}{PWV(t+\Delta t) + PWV(t)} >, 0 \leqslant f_{FD}(\Delta t) \leqslant 1 \quad (5)$$

which measures the characteristic range of relative changes as a function of the relative time Δt. Assuming a log-normal distribution of the data, the characteristic fluctuation time (τ_{FD}) and the growth rate (γ_{FD}) can be determined by fitting the observations to the following function:

$$< f_{FD}(\Delta t) > = < f_{FD}(\infty) > \times [1 - exp(-(\Delta t/\tau)^{\gamma})] \quad (6)$$

The $<f_{FD}(\Delta t)>$ should range from $<f_{FD}(0)>=0$ to a saturated value $<f_{FD}(\infty)>$. From the PWV time series for the ORM, we have computed the average normalized difference for the complete data set for Δt ranging from 0 to 72 hours in steps of 2 hours following equation 5 (see Fig. 7(a)). The characteristic time and the growth rate (τ and γ) have been determined by fitting the equation 6 to $<f_{FD}(\Delta t)>$ using a gradient-expansion algorithm (task CURVEFIT from the IDL Astronomy User's Library) and minimizing χ^2. The derived values are: τ = 46.28 hours, γ = 0.43, and $< f_{FD}(\infty) >$ =0.49 mm. The PWV at a time t+Δt will be, on average, within the range: PWV(t)×[1±$f_{FD}(\Delta t)$]. Let us assume that PWV=2.5 mm at a given time t, the PWV expected at a later time t±Δt (with Δt ranging from 0 to 72 hours) will be in the range between the two curves in figure 7(b).

The AD method was applied by Skidmore et al. (2009) to study the temporal variability of the seeing at the five candidate sites for the Thirty Meter Telescope (TMT). The AD method provides information of the absolute range of expected PWV at a time t+Δt knowing the PWV at a given time t. The AD is calculated over the entire data set simply applying:

$$f_{AD}(\Delta t) = < |PWV(t+\Delta t) - PWV(t)| > \quad (7)$$

The average $<f_{AD}(\Delta t)>$ over the entire data set derived from the PWV time series for the ORM is shown in figure 8(a). Let us again assumed that PWV(t)=2.5 mm, the PWV at a time t+Δt should be in the range between the two curves in figure 8(b).

According to figures 7(b) and 8(b), and considering Δt=24 hours, the PWV(t+24) should be in the range 1.86-3.14 mm using the FD approach or in the range 0.29-4.70 mm when the AD method is prefered. The AD method seems to be more restrictive than the FD method, but the reader should take into account that both procedures are averaging over a large number of data and the dispertion is large in both cases.

We have also calculated the average temporal range in which the PWV is always below a defined value PWV_0 (Fig. 9). We obtained that the average temporal range in which conditions are good or excellent for IR observations (PWV$\leqslant$ 3 mm) at the ORM is around 16.9 hours.

The three methods that were applied to study the temporal variability of the PWV represent statistical analysis of such temporal variations. A steep rise of the PWV in a short time scale can not be ruled out. Indeed, we found that differences larger than 1 mm in consecutive (two hours sampling) PWV measurements occur in ∼9% of the cases. This percentage decreases to ∼1.5% for differences larger than 2 mm in consecutive measurements. A significant improvement in PWV might also be possible. In the two-hour PWV time series for ORM, improvements larger than 1 mm or 2mm also occurs in ∼9% and ∼1.6% of the cases, respectively.

3.4 PWV statistics at Mauna Kea derived from GPS data

In order to compare the statistical results on PWV derived for ORM with a higher altitude site, we also carried out an

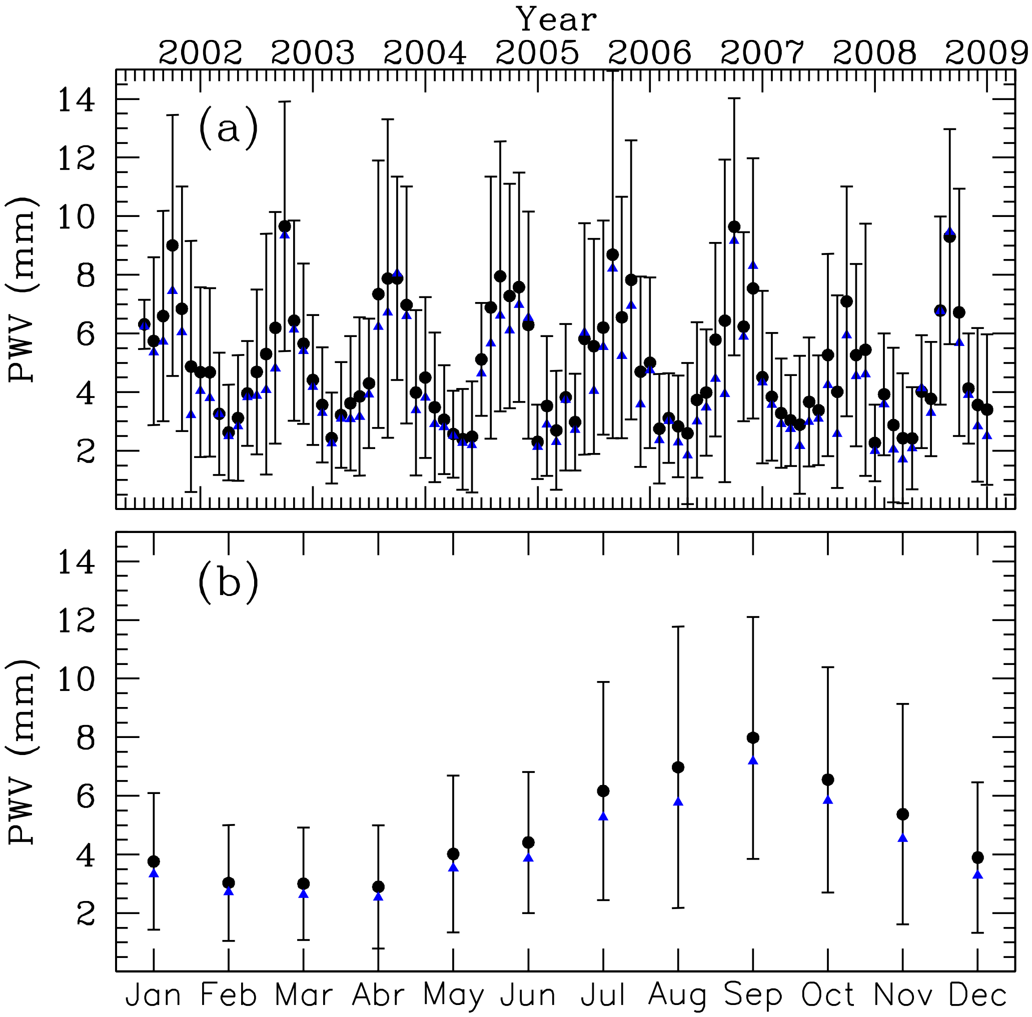

Figure 5. (a) Monthly statistical values of PWV for a 7.5-year period above ORM. This time series constitues a smoothed dataset of the two-hour time series derived from GPS measurements recorded at the ORM (including night and day data); (b) The monthly statistics of PWV for the period June 2001-December 2008 for ORM. In both plots, dots correspond to the average values and triangles to median values. Errorbars only indicate the standard deviation.

statistical analysis of PWV estimations derived from GPS measurement at a location closer to Mauna Kea observatory. Previous statistical results of PWV have been already obtained from other techniques (see e.g. Sayers et al. (2009); García-Lorenzo et al. (2009)) . In section §3.5 we will summarize PWV statistics for different worldwide astronomical sites obtained from data recorded using different techniques.

Table 2 presents the statistical results of the PWV time series derived from GPS measurements for the period from June 2001 to December 2008 at four km distant from Mauna Kea observatory. The global average PWV at Mauna Kea is almost 2 mm smaller than the corresponding mean PWV at ORM, which is not surprising due to the large difference in altitude between both sites (more than 1300 m). Statistically, Summer and Autumn present slightly larger PWV at Mauna Kea than Winter and Spring. However, a clear seasonal trend in the PWV behaviour is not clear from figures 10(a) and 10(b). The PWV is statistically smaller than 3 mm in 63% of the time (night+day), being this value almost independent of the season, although during spring nighttime the percentage increases to 70%. PWV measurements larger than 6 mm appear around 12% of the time at any season. The average temporal range in which conditions are good or excellent for IR observations (PWV$\leqslant$ 3 mm) at Mauna Kea is 23.4 hours (see figure 9).

Comparing tables 1 and 2, we can deduce that for each 10 hours of usefull nighttime for IR observations (PWV $\leqslant$ 3mm) at Mauna Kea, the ORM will present 6 useful hours. During Summer and Autumn, only 3.9 and 4.7 hours are useful for IR observations at ORM for each 10 useful hours at Mauna Kea, whereas during Winter and Spring these figures increase to 7.9 and 7.4 useful hours, respectively, for each 10 hours at Mauna Kea. Fair or mediocre conditions for IR observations (3mm $\leqslant$ PWV $\leqslant$ 6 mm) differ in around 10% when comparing results from Mauna Kea and ORM, being in any case larger at ORM. During Winter and Spring, ORM presents approximately the same percentage of bad conditions (PWV $\geqslant$ 10 mm) than the percentage at Mauna Kea

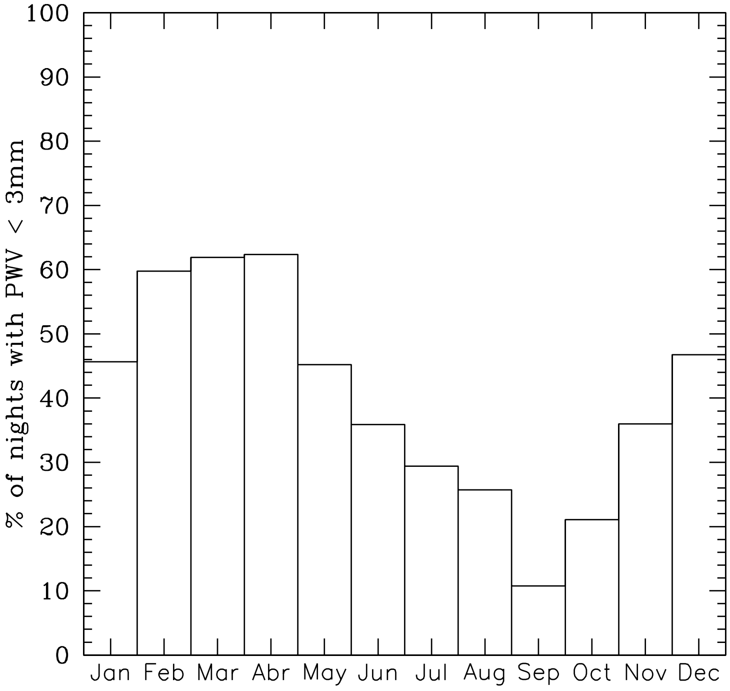

Figure 6. Monthly percentage of night time at which PWV $\leqslant$ 3 mm for the period June 2001-December 2008 at the ORM.

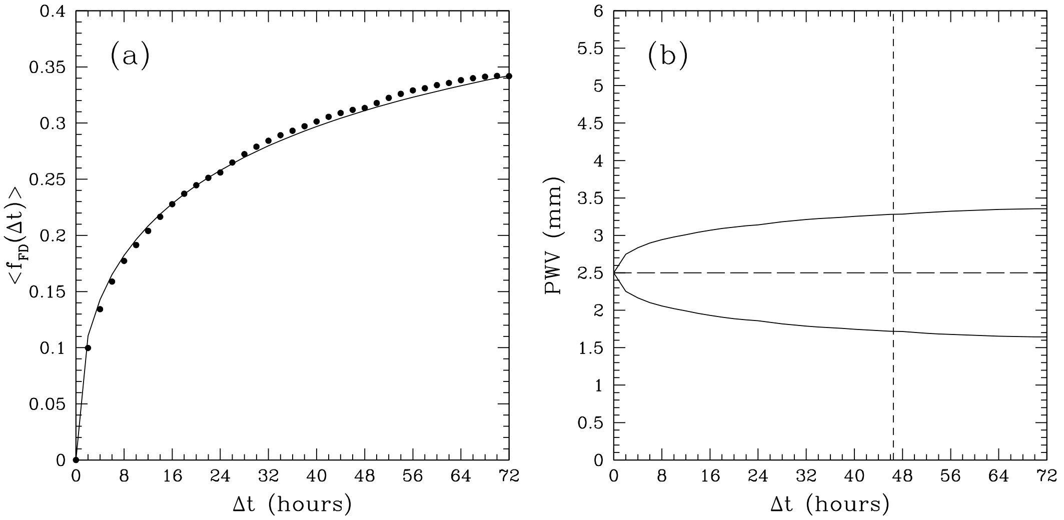

Figure 7. (a) Fractional difference of the PWV measurements as a function of the time interval averaged over the full data set. The standard deviation of the $<f_{FD}(\Delta\ t)>$ is 0.22 in average. (b) PWV range expected (continua lines) at $t+\Delta t$ when assuming a PWV(t)=2.5 mm (long-dashed line) applying the FD method. The short-dashed line indicates the characteristic time τ.

along the seasons. Moreover, the average temporal range in which conditions are stably excellente or good (PWV$\leqslant$ 3 mm) are similar (within uncertainties) at Mauna Kea and ORM.

This comparison demostrates that excellent conditions for IR astronomical observations, in terms of percentage and stability, are also possible in sites at relative low altitude (over 2000 m above sea level). This result might be related to the role of the troposphere thickness instead of the site altitude in the IR quality of a particular astronomical site (García-Lorenzo et al. 2004). Indeed, the seasonal behaviour of the PWV at ORM follows a quite similar behaviour than the troposphere thickness at this site (see figure 5 in García-Lorenzo et al. (2004)).

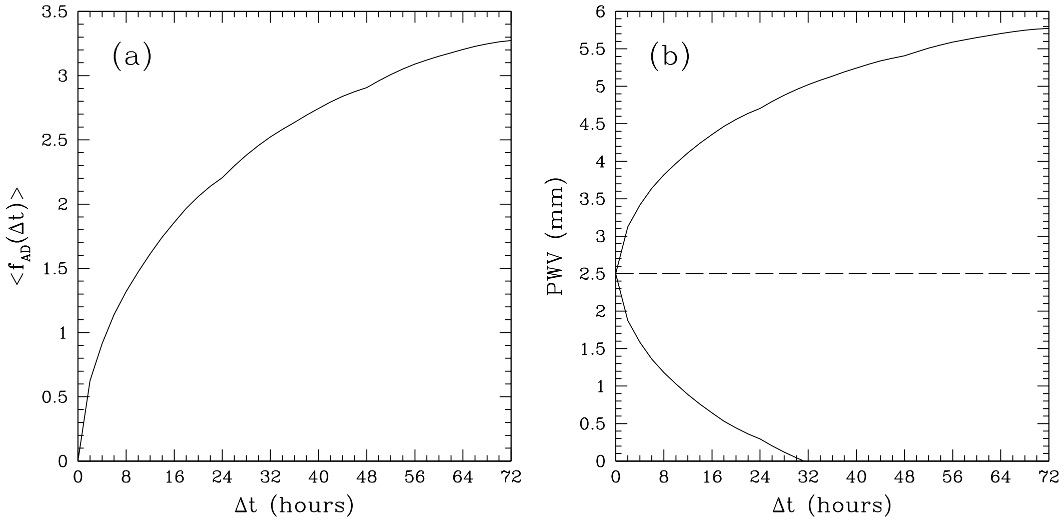

Figure 8. (a) Absolute difference of the PWV measurements as a function of the time interval averaged over the full data set. The average standard deviation of the data is 2.30 mm. (b) Expected range of PWV at any time t+Δt assuming a PWV equal to 2.5 mm (dashed line) at time t using the AD approach.

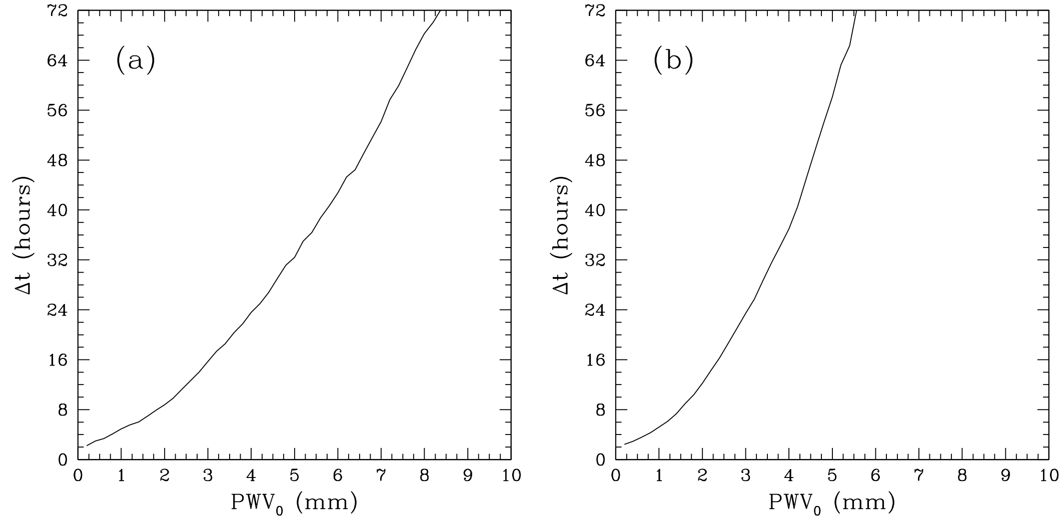

Figure 9. (a) Average temporal interval in which the PWV is lower than a defined PWV_0 value at ORM; (b) Average temporal interval in which the PWV is lower than a defined PWV_0 value at Mauna Kea.

3.5 Summary of PWV statistical results at astronomical sites

The comparison of PWV statistical results between astronomical sites is very complex due to the variety of techniques and procedure normally used. Different techniques provide different temporal coverages and samplings. Moreover, some of the techniques used to evaluate the water vapor content are strongly affected by rain and clouds (e.g. radiosondes and WVR). Others are only applicable near the zenith (e.g. radiometers), whereas GPS can provide continuous PWV estimates depite the effects of rain, dust or clouds. In spite of such differences, we summarize in table 3 statistical PWV results for different astronomical sites located at different altitudes above sea level. In the case of Mauna Kea, we have found median PWV values derived from four different techniques, showing significant discrepancies between the values. Even using the same database but different analysis period, statistical values may differ significantly. These differences also occur in the case of ORM, where Infrared sky radiance gives a significant lower PWV median than the other techniques used there. In both sites, GPS provides the largest PWV median value, as it is expected from the fact that GPS measures continuosly and under all weather conditions.

In order to calculate an approximate PWV median value comparable to that derived from the techniques affected by clouds, we have selected the GPS data recorded during photometric nights (clear nights from clouds and/or aerosol affecting astronomical observations). The atmospheric extinction coefficient – a measurement of the sky transparency – is measured at the ORM in the V (551 nm,

Table 2. Global and seasonal statistical results of precipitable water vapor (in mm) above Mauna Kea region including the percentage of time presenting a PWV value in a determined range.

		Global	**Winter**	**Spring**	**Summer**	**Autumn**
All:						
	Mean	3.0	2.8	2.7	3.1	3.2
	σ	2.4	2.50	2.2	2.2	2.6
	N	28607	5541	6897	8417	7752
	10%	0.6	0.3	0.5	0.8	0.6
	25%	1.2	0.9	1.2	1.5	1.3
	50%	2.3	1.9	2.1	2.6	2.3
	75%	4.1	4.1	3.7	4.2	4.3
	90%	6.5	6.7	5.9	6.2	7.4
All:	**PWV Range**					
	$<$ 2 mm	44%	52%	47%	36%	43%
	2-3 mm	19%	13%	19%	21%	19%
	3-6 mm	25%	22%	24%	32%	23%
	6-10 mm	11%	12%	9%	10%	13%
	$\geqslant$ 10 mm	1%	1%	1%	1%	2%
Day:						
	Mean	3.1	2.8	2.8	3.3	3.3
	σ	2.4	2.5	2.2	2.2	2.6
	N	16562	3072	4418	5141	3931
	10%	0.7	0.4	0.7	0.9	0.7
	25%	1.3	0.9	1.3	1.6	1.3
	50%	2.4	2.0	2.2	2.7	2.4
	75%	4.2	4.1	3.8	4.3	4.5
	90%	6.6	6.7	5.9	6.3	7.5
Day:	**PWV Range**					
	$<$ 2 mm	41%	50%	44%	33%	41%
	2-3 mm	19%	14%	21%	22%	19%
	3-6 mm	27%	23%	25%	34%	24%
	6-10 mm	11%	12%	9%	10%	14%
	$\geqslant$ 10 mm	2%	1%	1%	1%	2%
Night:						
	Mean	2.9	2.7	2.5	2.9	3.1
	σ	2.4	2.5	2.3	2.2	2.6
	N	12043	2462	2484	3276	3821
	10%	0.5	0.3	0.4	0.7	0.6
	25%	1.1	0.8	0.9	1.4	1.2
	50%	2.1	1.8	1.8	2.4	2.2
	75%	3.9	3.9	3.5	4.0	4.1
	90%	6.5	6.7	5.7	5.9	7.3
Night	**PWV Range**					
	$<$ 2 mm	48%	55%	53%	42%	45%
	2-3 mm	17%	12%	17%	19%	19%
	3-6 mm	23%	20%	21%	29%	22%
	6-10 mm	10%	12%	8%	9%	12%
	$\geqslant$ 10 mm	2%	1%	1%	1%	2%

K_V hereafter) and r' (625 nm) bands since 1984 by the Carlsberg Automatic Meridian Circle (CAMC). We have downloaded the atmospheric extinction coefficient for the period June 2001-December 2008 from the CAMC archive (http://www.ast.cam.ac.uk/d̃we/SRF/camc_extinction.html). We selected as photometric nights those satisfying the following requirements: (i) the total number of observing hours is larger than seven; (ii) the total number of photometric data taken is larger than 90% of the total number of observing hours; and (iii) the average K_V along the night is smaller than 0.2. 55% of the nights from June 2001 to December 2008 in the CAMC database follow the selection criteria. PWV measurements derived from GPS data during photometric nights were then used to derived the statistical values of PWV (see table 4).

Statistical values (average and median) of PWV strongly improve when specific weather conditions are selected, which is usually imposed by the techniques used to retrive PWV values. Therefore, the comparison of PWV values from different sites is only possible when the same tech-

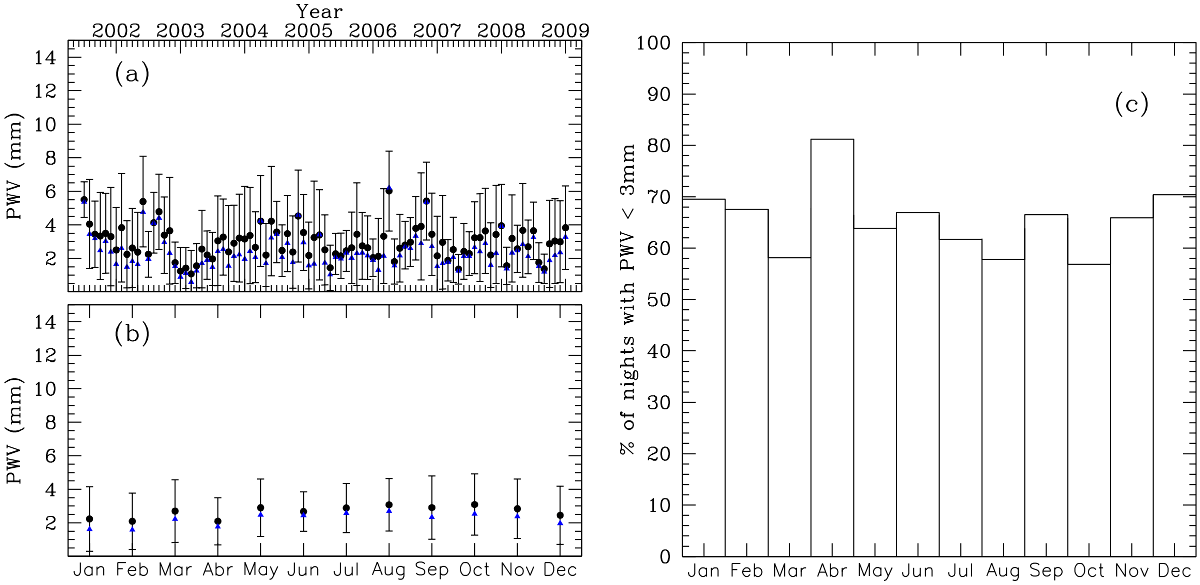

Figure 10. (a) Monthly average PWV values for a 7.5-year period above Mauna Kea. This time series constitues a smoothed dataset of the two-hour time series derived from GPS data close to Mauna Kea Observatory (including night and day data); (b) The monthly statistics of PWV for the period June 2001-December 2008 for Mauna Kea. In both plots, dots correspond to the average values and triangles to median values. Errorbars only indicate the standard deviation of the data; (c) Monthly percentage of night time at which PWV $\leqslant$ 3 mm at Mauna Kea for the period from June 2001 to December 2008.

Table 3. Statistical results of precipitable water vapor for different astronomical sites worldwide derived from different techniques and procedures.

Site	**Location: Lat, Lon**	**Height (m)**	**Median PWV (mm)**	**Technique**	**Temporal Range**	**Reference**
Las Campanas	29.01° S, 42.18° W	2200	2.8	225GHz-radiometer	2005/07-08	Thomas-Osip et al. (2007)
Cerro Tolar	21.96° S, 70.10° W	2290	4.02	GOES-8 satellite	1993/06-1996/02	Otárola et al. (2010)
			4.7	Surface PWV data	01/2004-12/2007	Otárola et al. (2010)
ORM	28.77° N, 17.88° W	2395	3.9	940nm-Radiometer	1996-1998	Kidger et al. (1998)
			3.9	GPS	2001/06-2008/12	this work
			2.6	IR Sky Radiance	2000-2002	Pinilla (2003)
La Silla	29.25° S, 70.73° W	2400	3.9	IR Sky Radiance	1983-1989	Sarazin (1990)
Paranal	24.63° S, 70.40° W	2635	2.3	IR Sky Radiance	1983-1989	Sarazin (1990)
San Pedro Mártir	31.04° N, 115.47° W	2830	2.63	GOES-8 satellite	1993/06-1996/02	Otárola et al. (2010)
			3.4	210GHz-radiometer	2006	Otárola et al. (2010)
Pico Veleta	37.07° N, 3.37° W	2850	2.9	940nm-Radiometer	1984-1987	Quesada (1989)
Cerro Armazones	24.58° S, 70.18° W	3064	2.87	GOES-8 satellite	1993/06-1996/02	Otárola et al. (2010)
			3.2	Surface PWV data	01/2004-12/2007	Otárola et al. (2010)
Dome C	75.06° S, 123.23° E	3233	0.34	Satellite & Model	2008	Saunders et al. (2009)
Mauna Kea	19.83° N, 155.47° W	4205	1.7	225GHz-radiometer	2001/06-2008/12	García-Lorenzo et al. (2009)
			1.2	Radiosondes	1983	Bely (1987)
			1.86	GOES-8 satellite	1993/06-1996/02	Otárola et al. (2010)
			2.1	225GHz-radiometer	01/2004-12/2007	Otárola et al. (2010)
			2.3	GPS	2001/06-2008/12	this work
Ridges A	81.5° S, 73.5° E	4053	0.21	Satellite & Model	2008	Saunders et al. (2009)
Dome A	80.73° S, 77.3° E	4083	0.23	Satellite & Model	2008	Saunders et al. (2009)
Cerro Tolonchar	23.93° S, 67.97° W	4480	1.7	GOES-8 satellite	1993/06-1996/02	Otárola et al. (2010)
			1.8	Surface PWV data	01/2004-12/2007	Otárola et al. (2010)
Chajnantor	23.02° S, 67.45° W	5080	1.0	Radiosondes	1998/10 & 2000/08	Giovanelli et al. (2001)
			1.2	225GHz-radiometer	1995/04-2000/04	Thomas-Osip et al. (2007)

Table 4. Seasonal statistical results of precipitable water vapor (in mm) above the Roque de los Muchachos Observatory derived from PWV estimations during photometric nights.

		Global	**Winter**	**Spring**	**Summer**	**Autumn**
Night:						
	Mean	3.9	3.2	3.1	4.7	4.5
	σ	2.6	1.9	1.9	2.9	2.8
	N	6146	1256	1517	2081	1292
	10%	1.2	0.9	0.9	1.7	1.4
	25%	2.1	1.7	1.7	2.6	2.3
	50%	3.4	2.8	2.9	3.9	4.0
	75%	5.2	4.2	4.2	6.2	6.2
	90%	7.3	5.7	5.7	8.4	8.3

nique and procedure have been used to adquire and analyse the data.

3.6 Infrared bands and PWV

ORM has been an astronomical site traditionally dedicated to optical and near-IR observations (from 0.4 to 2.5 μm). The 10 meters Gran Telescopio de Canarias will extend this range to the mid-IR, with CanariCam, a camera and spectrograph working in the thermal infrared between ~7.5 and 25 μm. In this section, we explore the implications in terms of atmospheric transmission of PWV values in the standard near and mid-IR windows in astronomy. We have modelled the theoretical near and mid-IR transmission spectrum for La Palma site using the ATRAN modelling software (Lord, S.D. 1992, NASA Technical Memor. 103957) throughout the web-based form at http://atran.sofia.usra.edu/cgi-bin/atran/atran.cgi . We selected the closest latitude to the site allowed (30 degrees), the altitude of the site (2400 m), scanning the PWV from 1 to 10 mm. The transmission spectrum derived from each PWV value was integrated in the spectral range covering the standard filters windows and these values were refered to the integrated transmission asumming a PWV equal to 1 mm (see table 5). The theoretical transmission spectrum for Mauna Kea was extracted from a model available at the GEMINI Observatory web pages (http://staff.gemini.edu/~kvolk/linkpage.html) which is also based on the ATRAN modeling software, although it is limited in PWV values. We followed the some procedure than in the case of La Palma, integrating the transmission spectrum in each filter window and refering the value to the derived for 1mm of PWV.

In both cases, similar results were found. The atmospheric transmission in bands H, K, and N decrease less than 5% for PWV variations from 1 to 10 mm. The atmospheric transmission in windows J, L, and M slowly decrease when PWV increase (up to 21% from 1 to 10 mm). The most significant effect occurs in band Q, where atmospheric transmission is around 50% smaller when PWV increase from 1 to 5 mm. When PWV is 10 mm, the atmospheric transmission is almost 35% of the transmission with 1 mm of PWV in Q-band. It is also important to note that high levels of water vapor also increase the thermal IR background, which is one of the major factors limiting the atmospheric transparency in mid-IR observations from ground-based sites. The effects of observing conditions (water vapor column, airmass, cloud cover, etc) in the quality of data recorded in mid-IR bands was illustrated in Mason et al. (2008) using real data obtained in Mauna Kea.

4 SUMMARY AND CONCLUSIONS

We have analised the water vapor content for the period from June 2001 to December 2008 above the ORM using PWV estimations from GPS data. We have verified the consistency of 940nm-radiometer and GPS estimation of PWV, removing the offset between both techniques. We have also presented statitical results for Mauna Kea for the same period, analysing the GPS close to Mauna Kea site with τ_{225GHz} measurements. Our main results and conclusions may be summarized as follows:

(i) The nighttime median PWV above ORM is 3.79 mm, with slightly differences between day and nighttime statistics.
(ii) The PWV presents a clear seasonal variation at the ORM. Winter and spring nights present the lower PWV statistics, with a median value of 2.82 mm and 2.86 mm, respectively.
(iii) More than 60% of the nighttime during February, March and April present good or excellent conditions in terms of water vapor (PWV $\leqslant$ 3 mm) at the ORM.
(iv) Comparing PWV statistical results for ORM and Mauna Kea, we deduce that for 10 hours of good conditions for IR observations at Mauna Kea during winter, the ORM will present 7.9 hours showing excellent conditions.
(v) The average temporal range presenting good or excellent conditions for IR observations (PWV $\leqslant$ 3mm) is comparable at ORM and Mauna Kea (16.9 hours and 23.4 hours, respectively).
(vi) The comparison of PWV at different astronomical sites is difficult because there is not an unique defined technique/procedure to estimate the PWV.

GPS is a promising technique to unify the PWV estimations at many astronomical sites.

ACKNOWLEDGMENTS

This paper is based on GPS data recor ded from the GPS station at the Roque de los Muchachos Observatory on the island of La Palma and from the labelled MKEA station at

Table 5. Atmospheric transmission as a function of PWV relative to the atmospheric transmission extracted for 1 mm of PWV for the standard near and mid infrared bands.

Near La Palma	**PWV** (mm)	**Filter J** (1.1-1.4 μm)	**Filter H** (1.5-1.8 μm)	**Filter K** (2.0-2.4 μm)	**Filter L** (3.0-4.0 μm)	**Filter M** (4.5-5.1 μm)	**Filter N** (10-12 μm)	**Filter Q** (17.5-22.5 μm)
	1.5	97.4	99.7	99.8	97.5	97.5	99.8	89.3
	3.0	92.5	98.8	99.1	92.2	91.8	99.4	68.2
	5.0	88.7	98.1	98.4	87.9	87.2	99.0	54.7
	6.5	86.8	97.6	97.9	85.6	84.9	98.8	48.9
	7.6	85.8	97.4	97.7	84.4	83.9	98.7	47.2
	10.0	83.2	96.7	96.9	80.9	79.4	98.3	36.5
Mauna Kea	**PWV** (mm)	**Filter J** (1.1-1.4 μm)	**Filter H** (1.5-1.8 μm)	**Filter K** (2.0-2.4 μm)	**Filter L** (3.0-4.0 μm)	**Filter M** (4.5-5.1 μm)	**Filter N** (10-12 μm)	**Filter Q** (17.5-22.5 μm)
	1.5	98.6	99.8	99.9	99.0	98.8	99.1	84.8
	3.0	91.1	98.7	99.1	93.3	92.2	98.2	68.3
	5.0	87.2	97.9	98.4	89.7	88.1	96.9	55.9
	6.5	86.1	97.6	98.6	89.0	88.0	—	—

Mauna Kea on the island of Hawaii. Both GPS stations are part of the international network of GPS stations EUREF (www.euref.eu).

Measurements of the 225 GHz optical depths at Mauna Kea were recorded from the web page of the Caltech Submillimeter Observatory (CSO) (http://puuoo.submm.caltech.edu/). The coefficient-extinction data were downloaded from the database (http://www.ast.cam.ac.uk/~dwe/SRF/camc_extinction.html) of the Carlsberg Meridian Circle of the Isaac Newton Group on.

Thanks are due to M. Kidger who managed the water vapor monitoring campaigns at the ORM from 1996 to 2002. The authors also thank I. Romero from Canary Islands Advanced Solutions (http://www.sacsl.es/) and J.A. Acosta-Pulido from Instituto de Astrofísica de Canarias for stimulating discussions and help. Finally, we wish to thank the referee for very constructive comments and suggestions.

This work was partially funded by the Instituto de Astrofísica de Canarias and by the Spanish Ministerio de Educación y Ciencia (AYA2006-13682 and AYA2009-12903). This work has been carried out within the framework of the European Project OPTICON and under Proposal FP6 for Site Selection for the European ELT. B. García-Lorenzo and A. Eff-Darwich thank the support from the Ramón y Cajal program by the Spanish Ministerio de Educación y Ciencia.

REFERENCES

American Meteorological Society (AMS), Glossary of Meteorology, 2nd ed., Boston, Mass, 2000

Altamimi, Z., Collilieux, X., Legrand, J., Garayt, B., & Boucher, C. 2007, Journal of Geophysical Research (Solid Earth), 112, 9401

Askne, J., & Nordius, H. 1987, Radio Science, 22, 379

Bely, P.-Y. 1987, PASP, 99, 560

Bevis, M., Businger, S., Chiswell, S., Herring, T. A., Anthes, R. A., Rocken, C., & Ware, R. H. 1994, Journal of Applied Meteorology, 33, 379

Bevis, M., Businger, S., Herring, T. A., Rocken, C., Anthes, R. A., & Ware, R. H. 1992, Journal of Geophysical Research, 97, 15787

Blewitt, G. 1998, GPS for Geodesy, Springer-Verlag, pp 231-270

Boccolari, M., Fazlagi, S., Santangelo, R. 2006, Annals of Geophysics, Vol. 49, Num. 4/5, pp 881/889

Boehm, J., Heinkelmann, R., & Schuh, H. 2007, Journal of Geodesy, 81, 679

Chamberlin, R. A., & Bally, J. 1994, Applied Optics, 33, 1095

Cohen, M., Walker, R. G., Barlow, M. J., & Deacon, J. R. 1992, AJ, 104, 1650

Davis, G. R., Naylor, D. A., Griffin, M. J., Clark, T. A., & Holland, W. S. 1997, Icarus, 130, 387

Emardson, T. R., Johansson, J., & Elgered, G. 2000, IEEE Transactions on Geoscience and Remote Sensing, 38, 324

Ferrare, R., Brasseur, L., Clayton, M., Turner, D., Rerner, L., & Gao, B.-C. 2002, Evaluation of TERRA aerosol and water vapour measurements using ARM SGP data, paper presented at American Meteorological Society 11th Conference on Atmospheric Radiation, Ogden, Utah, 3-7 June 2002

Gao, B.-C., Goetz, A. F. H., Westwater, E. R., Conel, J. E., & Green, R. O. 1993, Journal of Applied Meteorology, 32, 1791

García-Lorenzo, B., Castro-Almazán, J. A., Eff-Darwich, A., Muñoz-Tuñón, C., Pinilla-Alonso, N., Rodriguez-Espinosa, J. M., & Romero, I. 2009, Proc.SPIE, 7475, 42

García-Lorenzo, B. M., Fuensalida, J. J., & Eff-Darwich, A. M. 2004, Pproc. SPIE, 5572, 384

Ge, M., Calais, E., & Haase, J. 2000, Geophysical research Letters, 27, 1915

Giovanelli, R., et al. 2001, PASP, 113, 803

Hammersley, P. L. 1998, New Astronomy Review, 42, 533

Jin, S., Luo, O. F., & Gleason, S. 2009, Journal of Geodesy, 83, 537

Kelly, B. C. 2007, ApJ, 665, 1489

Kenyeres, A., & Bruyninx, C. 2004, AGU Fall Meeting Abstracts, A115

Kidger, M. R., Rodríguez-Espinosa, J. M., del Rosario, J. C., & Trancho, G. 1998, New Astronomy Review, 42, 537

Kidger, M., Pinilla, N., & Espinosa, J. 2002, Astronomical Site Evaluation in the Visible and Radio Range, 266, 220

Kleijer, F. 2001, Physics and Chemistry of the Earth A, 26, 467

Leick, A. 2004, GPS Satellite Surveying, Third Edition, Published by John Wiley & Sons, Inc.

Li, Z., Muller, J.-P., & Cross, P. 2003, Journal of Geophysical Research (Atmospheres), 108, 4651

Liou, Y.-A., Teng, Y.-T., van Hove, T., & Liljegren, J. C. 2001, Journal of Applied Meteorology, 40, 5

Liu, Z-Y. 1985 User's Manual, Electronics Division Internal Rep. 271 (National Radio Astronomy Observatory, Socorro, New Mexico

Mason, R., Wong, A., Geballe, T., Volk, K., Hayward, T., Dillman, M., Fisher, S., & Radomski, J. 2008, Proc.SPIE, 7016,

McKinnon, M. 1987, Measurement of Atmospheric Opacity Due to Water Vapor at 225 GHz, Millimeter Array Memo 40 (National Radio Astronomy Observatory, Socorro, New Mexico, 1987)

Mountain, C. M., Leggett, S. K., Selby, M. J., & Zadrozny, A. 1985, A&A, 150, 281

Muñoz-Tuñón, C., Varela, A. M., & Fuensalida, J. J. 2007, Revista Mexicana de Astronomia y Astrofisica Conference Series, 31, 36

Munoz-Tunon, C., Vernin, J., & Varela, A. M. 1997, A&AS, 125, 183

Niell, A. E., Coster, A. J., Solheim, F. S., Mendes, V. B., Toor, P. C., Langley, R. B., & Upham, C. A. 2001, Journal of Atmospheric and Oceanic Technology, 18, 830

Otárola, A., Travouillon, T., Schöck, M., Els, S., Riddle, R., Skidmore, W., Dahl, R., Naylor, D., & Querel, R. 2010, PASP, accepted

Pinilla, N., Kidger, M., & Espinosa, J.M. 2002, Astronomical Site Evaluation in the Visible and Radio Range, 266, 216

Pinilla, N. 2003, Research report to obtain the degree "Diploma de Estudios Avanzados", Astrophysics department, Universidad de La Laguna (noe.pinillaalonso@gmail.com)

Quesada, J. A. 1989, PASP, 101, 441

Racine, R. 1996, PASP, 108, 372

Romero, I., Boomkamp, H., Dow, J., & Garcia, C. 2003, Advances in Space Research, 31, 1911

Saastamoinen, J. 1973, Bull. Géod., Nouvelle Sér., Année 1973, No. 107, p. 13 - 34, 107, 13

Saastamoinen, J. 1972, The Use of Artificial Satellites for Geodesy, 15, 247

Sarazin, M. 1990, VLT Report 62, VLT Site Selection Working Group Final Report, Nov.14 (see also http://www.eso.org/gen-fac/pubs/astclim/)

Saunders, W., et al. 2009, PASP, 121, 976

Sayers, J., et al. 2009, arXiv:0904.3943

Schneider, M., Romero, P.M., Hase, F., Blumenstock, T., Cuevas, E., & Ramos, R. 2009, Atmos. Meas. Tech. Discuss., 2, 1625-1662

Skidmore, W., Els, S., Travouillon, T., Riddle, R., Schöck, M., Bustos, E., Seguel, J., & Walker, D. 2009, PASP, 121, 1151

Thomas-Osip, J., McWilliam, A., Phillips, M. M., Morrell, N., Thompson, I., Folkers, T., Adams, F. C., & Lopez-Morales, M. 2007, PASP, 119, 697

Yagai, I. 2002, AGU Fall Meeting Abstracts, 103

Zhang, G., Vivekanandan, J., & Politovich, M.K. 1999, in Eighth Conf. on Aviation, Range, and Aerospace Meteorology, Dallas, TX, Amer.Meteor.Soc., 497-501

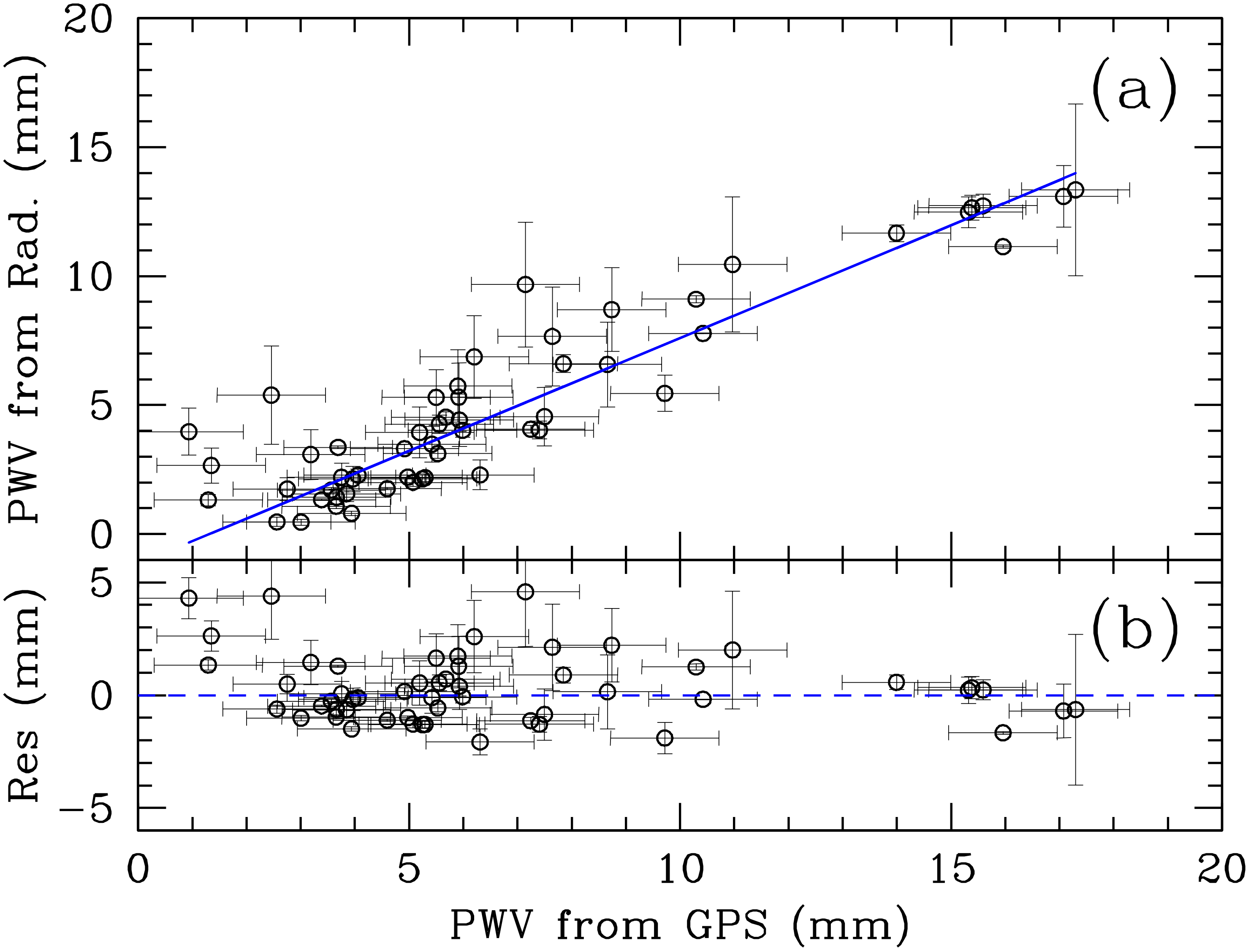
(a)
(b)
PWV from Rad. (mm)
Res (mm)
PWV from GPS (mm)
0
5
10
15
20
−5

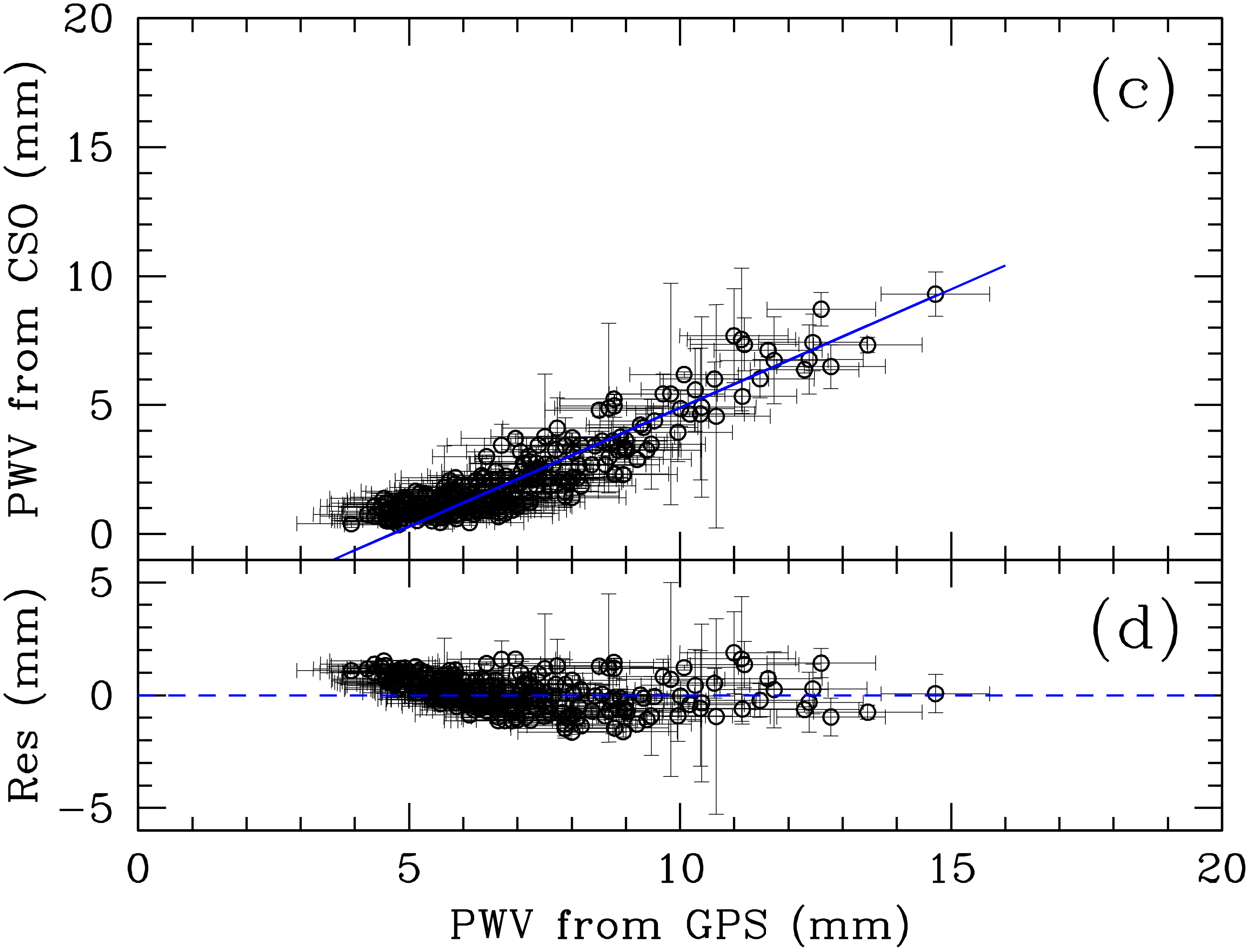

(c)
(d)
PWV from CSO (mm)
Res (mm)
PWV from GPS (mm)
0
5
10
15
20
−5